Measurement of contact angle and work of adhesion at high temperature

N. EUSTATHOPOULOS
INPG, LTPCM-ENSEEG, BP. 75, 38402 Saint Martin d'Heres, France
E-mail: nikos@ltpcm.inpg.fr

N. SOBCZAK
Foundry Research Institute, 73 Zakopianska St., Cracow, Poland
E-mail: natalie@iod.krakow.pl

A. PASSERONE
IENI-CNR, Via de Marini, 6, 16149, Genoa, Italy
E-mail: a.passerone@ge.ieni.cnr.it

K. NOGI
JWRI, Osaka University, 11-1 Mihogaoka, Osaka 567-0047, Japan
E-mail: nogi@jwri.osaka-u.ac.jp

A critical review is given of the present state of knowledge and future perspectives in high-temperature contact angle measurement. Experimental results obtained by the different versions of the sessile drop method and by various procedures are given in order to illustrate the two main sources of scatter in wettability data, the first being related to the quality of the substrates and the second to control of the furnace atmosphere.
© *2005 Springer Science + Business Media, Inc.*

1. Introduction

The Young contact angle θ_Y is a unique characteristic of a solid-liquid-vapour system. Its value quantifies the intrinsic aptitude of a non-reactive liquid to spread on a flat, undeformable, perfectly smooth and chemically homogeneous solid surface. Measurements of θ_Y and of the liquid surface tension σ make it possible to evaluate the Dupré work of adhesion $W_a = \sigma(1 + \cos\theta_Y)$, a quantity that characterises the thermodynamic stability of interfaces between dissimilar materials and is widely used in practice for predicting their potential bonding properties. Moreover, θ_Y enters into all model equations describing the wetting of liquids on real solid surfaces, i.e., surfaces with a certain roughness and degree of heterogeneity.

Despite the apparent simplicity of sessile drop experiments, the experimental evaluation of reliable θ_Y values at high temperatures remains a major problem and a serious obstacle to the development of scientific approaches to wetting phenomena. This is evidenced by a particularly large level of inter-laboratory scatter in reported θ values. For instance, contact angle values for molten copper on alumina measured in eight different laboratories between 1959 and 1987 range from 110° to 170°, corresponding to adhesion energies differing by a factor of 40! [3]. More recently, using high-purity α-alumina single crystals (SC) and high-purity gases or high-vacuum furnace environments, the scattering of experimental values on the Cu/alumina system has been significantly reduced. However, while in metal/ceramic systems the experimental error on θ is only 1–3°, the values of this quantity measured "for the same system" by various teams still differ by 17° [1–7] (Table I). This corresponds to a scattering of work of adhesion values as high as 75%. Scattering is even greater with polycrystalline (PC) non-oxide but oxidisable ceramics presenting a range of non-stoichiometry such as TiN [8–12] (Table II) and TiC [12]. A similar very wide scatter of data is also observed for a highly oxidisable metal such as Al on alumina [13, 14] or AlN substrates [15].

The above examples illustrate an important feature of wettability experiments, namely their poor repeatability. This is caused by chemical heterogeneities and by the roughness of real solid surfaces resulting in hysteresis of the contact angle. Hysteresis is defined by the difference $\theta_a - \theta_r$ between the advancing contact angle measured after spreading of the liquid on the surface and the receding contact angle reached when the liquid retreats, with $\theta_a > \theta_Y > \theta_r$. Hysteresis is due to the existence of metastable states at the vicinity of the triple line, each of which corresponds to a possible microscopic contact angle. For a given solid/liquid/vapour system, substrate preparation, and method of measurement, the observed θ_a(or θ_r) value also depends on vibrations in the system, a factor that can be hard to control. Differences in substrate preparation and/or in the furnace atmosphere help to amplify the dispersion of inter-laboratory θ measurements. Finally, the surface energies of metals and non-oxide ceramics are known

TABLE I Contact angle of pure copper on $\alpha M\text{Al}_2\text{O}_3^{\text{SC}}$ measured by the sessile drop technique (except [2], immersion-emersion technique)

| T (°C) | Conditions | | ($\theta°$) | Ref. |
	Atmosphere	Roughness, orientation		
1150	hv ($7\cdot10^{-4}$ Pa)		129	Naidich, 1981 [1]
1100	He-H$_2$; $P_{O2} = 10^{-22}$ Pa		127*	Ownby and Liu, 1988 [2]
1150	hv (10^{-4} Pa); Ar-H$_2$	$R_a = 15$ nm; random	131	Li et al., 1988 [3]
1100	hv (10^{-4} Pa)	$R_a = 8$ nm; random	126	de Jonghe et al., 1990 [4]
1100	hv (10^{-4} Pa)	$R_a = 3$ nm		Vikner, 1993 [5]
		random	128	
		$1\bar{1}02$	120	
		0001	123	
1098	Various buffer gases	$R_a < 10$ nm; random		Ghetta et al., 1996 [6]
	$10^{-23} < Po_2 < 10^{-17}$ Pa		130	
	$10^{-16} < Po_2 < 10^{-11}$ Pa		118	
1150	Gettered Ar		114	Saiz et al., 1998 [7]

*—plateau value; hv—high vacuum

TABLE II Contact angles of pure copper on nominally stoichiometric sintered TiN$^{\text{PC}}$ measured by the sessile drop technique

| T (°C) | Conditions | | ($\theta°$) | Ref. |
	Atmosphere	Roughness		
1120	hv (10^{-1} Pa)		126	Kotsch, 1967 [8]
1150	hv (10^{-3} Pa) + Ti getter		110	Xiao and Derby, 1995 [9]
1100	hv (10^{-3} Pa) + Ta chamber	$R_a = 50$–100 nm	50–60	Lequeux et al., 1998 [10]
1167	He–H$_2$; $Po_2 = 10^{-9}$ Pa	$R_a = 50$ nm	98	Muolo et al., 2001 [11]
1100	N$_2$-H$_2$	$R_a = 16$ nm	96	Kalogeropoulou et al., 2001 [12]

to depend strongly on the composition of the vapour phase, especially oxygen. As a consequence, small uncontrolled variations of the activity of this element can cause a significant change in θ, thus increasing the scatter of wetting data.

The aim of this review is, after a brief recall of the main techniques of contact angle measurements (Section 2), to examine and illustrate the above two main sources of scattering of high-temperature wettability data: the first being related to the quality (i.e., purity and crystallinity) and preparation of the substrates (Section 3) and the second, to the control of furnace atmosphere (Section 4). The 5th section is devoted to the measurement of surface tension of the liquid. Only non-reactive systems are considered.

2. Types of equipment for contact angle measurements at high temperature

The technique most widely used for wetting experiments at high temperatures is the sessile drop method. In its classical form, shown in Fig. 1a, a small piece of solid sessile drop material, typically some tens or hundreds of mg, is placed on a microscopically flat substrate and then heated above its melting temperature. Although this method is usually employed to obtain advancing contact angles, it may also lead to receding contact angles, by increasing the ratio of the solid base diameter to solid height. In another variant, a metal or alloy is melted in an unwetted and chemically inert closed ceramic tube and is then dispensed on the substrate surface through a small hole in the tube end by applying a back-pressure of inert gas (Fig. 1b) or using a piston. One advantage of this second technique
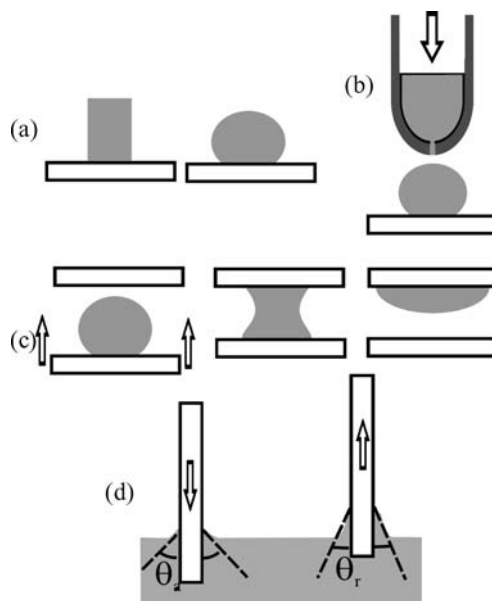

Figure 1 Methods of measurements of contact angle by different versions of sessile drop method (a–c) and by the tensiometric immersion-emersion technique (d).

is that oxide films on liquid metals are disrupted during dispensing.

In the "transferred drop" technique a sessile drop can be melted on an inert substrate, which is then raised so that the top surface of the drop contacts a fresh solid surface and subsequently lowered (Fig. 1c). Liquid can be transferred to the top substrate provided this is better wetted than the donor. In all of the above techniques θ_a values are measured and are attained by an irreversible movement of the triple line from $\theta \approx 180°$ to θ_a. This
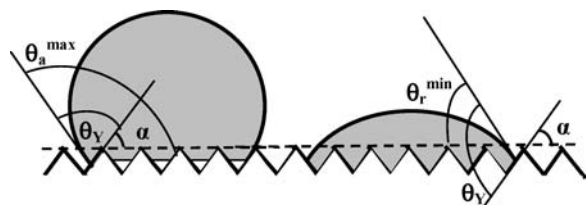
Figure 2 Maximum advancing (θ_a^{max}) and minimum receding (θ_r^{min}) contact angles on a rough surface.

minimises the difference $\theta_a - \theta_Y$ between the observed and intrinsic contact angles.

A very different method is the tensiometric "immersion-emersion" technique (Fig. 1d), which gives both θ_a (during immersion) and θ_r (during emersion). For non-wetting liquids, θ_a and θ_r are attained by a slow deformation of the liquid surface during the movement of the solid plate or cylinder. As a consequence, these values are much closer to the upper θ_a^{max} and lower θ_r^{min} limits of the hysteresis domain, respectively, than in the cases of irreversible wetting.

3. Effects of substrate quality

What is the greatest accuracy expected of θ_Y determinations in the field of high temperature materials? Important information on this question was provided by the study of de Jonghe *et al.* [4], who measured θ_a and θ_r angles by the immersion-emersion technique in high vacuum for various non-reactive metals using high-purity monocrystalline α-alumina cylinders. For this type of solid, for which it is reasonable to suppose that hysteresis results mainly from roughness, the upper θ_a^{max} and lower θ_r^{min} limits of hysteresis are related to the maximum slope α_a^{max} of the surface profile by the equations [16] (Fig. 2):

$$\theta_a^{max} = \theta_Y + \alpha^{max}, \quad \theta_a^{min} = \theta_Y - \alpha^{max} \qquad (1)$$

Fig. 3a illustrates the results of de Jonghe *et al.* for a pure Sn/Al$_2$O$_3$ system plotted as a function of average

roughness R_a and as a function of the ratio R_a/λ_a (λ_a being the average wavelength of the asperities), a quantity, which is proportional to the average slope of the substrate surface profile. It is seen that with increasing R_a, the $\theta_a - \theta_r$ first increases rapidly, then for about $R_a > 500$ nm, hysteresis starts to decrease and tends to zero as the liquid/solid interface is transformed to a "composite" interface (partially solid/vapour and partially solid/liquid). The important point here is that $\theta_a - \theta_r$ values as low as a few degrees can be attained by using very smooth surfaces (R_a of a few nm). In this example a θ_Y value of 128° was evaluated with an accuracy of $\pm 3°$. Note that for $R_a = 500$ nm, θ_a exceeds θ_Y by nearly 30°.

The results of de Jonghe *et al.* agree with those of Hitchock *et al.* [17], who evaluated θ_Y values for several liquid metals on ceramic substrates by extrapolating to zero roughness the θ_a vs R_a/λ_a experimental curve obtained using the classical sessile drop technique. An example is given in Fig. 3b for Hg on vitreous carbon surfaces prepared by abrasion with $1\text{nm} < R_a < 500$ nm. According to this and other results obtained by Hitchock *et al.* using substrates with a random roughness no higher than a few nanometers, the error on the value of the intrinsic contact angle due to roughness becomes negligible for this type of solids in comparison with other sources of error, for instance the error associated with the method used to calculate the contact angle from the droplet profile. For random roughness surfaces with R_a of about 100 nm, the excess ($\theta_a - \theta_Y$) values are still a few degrees while for the rougher substrates studied by Hitchock *et al.*, with R_a values close to 1 μm, the excess ($\theta_a - \theta_Y$) values measured for various non-wetting liquids were close to 20°. Naidich *et al.* obtained similar results for various low-melting point metals (Pb, Sn, In) on quartz substrates in high vacuum [18]. For these non-wetting systems, the authors found that the advancing contact angles on rough substrates ($R_a \approx 1250$ nm) exceed those on smooth quartz surfaces by 15–40°, depending on the metal.
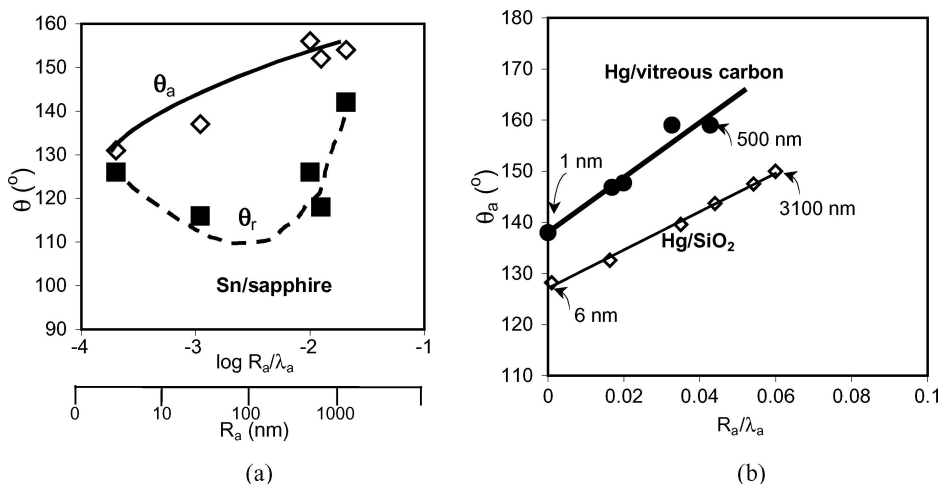

(a)

(b)

Figure 3 (a) Advancing θ_a and receding θ_r contact angles measured by the immersion-emersion method for the Sn/monocrystalline alumina system [4], plotted as a function of average roughness R_a and of logarithm of R_a/λ_a; (b) θ_a vs R_a/λ_a relationships for Hg obtained by the sessile drop technique on abraded silica and vitreous carbon; the arrows indicate the average roughness R_a [17].

T A B L E   I I I   Contact angles of non-reactive Cu-25 at% Si alloy on Si and C faces of (0001) plane of $\alpha - SiC^{SC}$ in He microleaks $P = 5 \cdot 10^{-8}$ atm at $T = 1150°C$ (the droplet mass is about 50 mg). The contact angles are obtained by a tangent method or (in parenthesis) from the linear dimensions of the sessile drop assuming a spherical shape [19]

	Contact angle, $\theta(°)$			
Substrate	1st exp	2nd exp	3rd exp	Average
face Si	32.6 ± 0.7	33.8 ± 0.4	33.8 ± 1.6	33.4 ± 0.8
	$[31.8 \pm 0.8]$	$[31.9 \pm 0.8]$	$[29.8 \pm 1.4]$	$[31.2 \pm 1.4]$
face C	43.1 ± 0.5	42.5 ± 0.8	42.5 ± 0.9	42.7 ± 0.4
	$[41.0 \pm 0.7]$	$[40.0 \pm 1.0]$	$[40.3 \pm 1.5]$	$[40.4 \pm 0.6]$

From the above studies it can be concluded that using high purity monocrystalline or amorphous substrates with a random roughness no higher than a few nanometers, advancing contact angles equalling θ_Y to within a few degrees can be measured. With such substrates a high repeatability is expected. An example is given in Table III for a non-reactive Cu−Si alloy on the two polar surfaces of a basal plane of $\alpha - SiC$ with $R_a = 1$–2 nm [19]. As shown in this table, the main uncertainty on contact angles is not due to the scatter of the experimental values of θ_a measured in successive experiments (less than $1°$) but rather to the method used to deduce θ_a from the sessile drop profile (about $2°$). The high repeatability attained in these experiments led to the conclusion that wetting by a Cu silicide of the two polar surfaces of hexagonal SiC differs by about $10°$.

When oxide substrates are used, a further factor affecting wetting is adsorption of OH groups. When the content in OH groups of oxide surfaces is high, as after an hydroxylation treatment, initial contact angles as high as 160–$180°$ can be obtained, as indeed observed for Au on sapphire [20] or on silica [21]. After removing these groups, occurring during holding in a vacuum at $T > 1000°C$, the contact angles in the above systems decrease by several decades.

As for inter-laboratory dispersion, the contact angle of molten gold on single crystals of smooth surface alumina measured by six different teams ranged between $131°$ and $140°$ [13], which is an acceptable dispersion around an average value of $135°$. The corresponding uncertainty in the work of adhesion is $\pm 17\%$. If met-als with a higher affinity for oxygen than Au are used, such as Cu and Ni, the scatter of contact angles measured in different laboratories is higher (see, Table I and Section 4).

Ceramics of high technological interest can seldom be obtained as the high-purity monocrystalline specimens desirable for Young contact angle measurements. The presence of grain boundaries in substrates used in sessile drop experiments causes several complications. Fig. 4a shows results obtained by Li *et al.* [22] for molten copper on both mono- and polycrystalline $\alpha -$ alumina substrates by the classical sessile drop technique [3]. The θ_a values measured on alumina single crystals with $R_a = 15$ nm ranged between $128°$ and $134°$ while with polycrystalline substrates the contact angles lay between $160°$ and $130°$. It was shown that this poor repeatability is not due to the increased average random surface roughness of polycrystalline substrates but rather to localized defects, which can affect wetting even if they do not modify significantly the average roughness characteristics. Such defects are holes caused by decohesion of grains during mechanical polishing, or pores of micron size often present in sintered material, or even scratches (Fig. 4b). All these are "strong" defects, i.e., they can easily pin the triple line and prevent spreading. Note that the use of polycrystals can also lead to increasing roughness by grain boundary grooving, a process which occurs rapidly on metallic surfaces at temperatures higher than a half of the melting point of the metal. For ceramics this process can increase significantly the surface roughness at $T > 1500°C$ [23, 24].
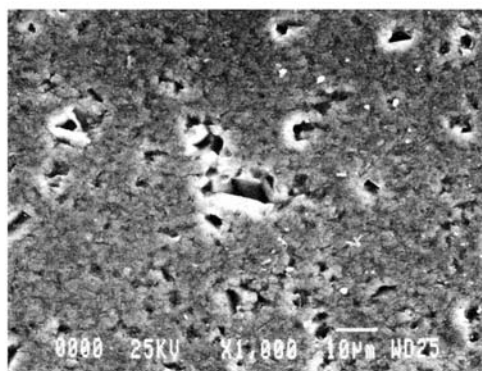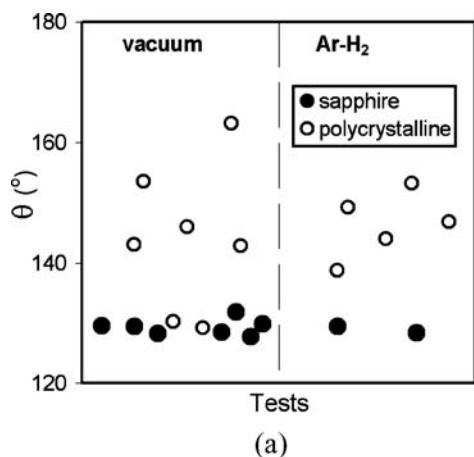

Figure 4 (a) Contact angle values of Cu on sapphire ($R_a = 15$ nm) and polished polycrystalline alumina substrates ($R_a = 50 \pm 20$ nm) at 1150°C in vacuum and Ar-H$_2$ atmosphere measured by the same procedure in different experiments [3]; (b) SEM image of polished polycrystalline alumina surface showing pores and holes due to detachment of grains during polishing [22].

A major disadvantage of sintered ceramics is their low purity. This is due to impurities contained in the initial powder or introduced into the material involuntarily in the course of processing or yet again due to additives promoting sintering. In many cases additives are present as second phases located at grain boundaries or triple junctions and their volumetric concentration can attain several per cent.

Experimental studies performed for composite (two-phase) surfaces [25, 26] have shown that in this range of volumetric concentrations the influence of second phases on advancing contact angles of the solid matrix is very limited (a few degrees). A more important effect can result from the segregation of impurities at the solid surface and liquid/solid interface. At high temperatures, this segregation can occur by rapid diffusion along the grain boundaries, thus affecting wettability even in short-time experiments. For instance, segregation at the Cu/TiN interface of Fe, introduced into sintered TiN during the milling process, caused an unexpected transition from non-wetting to wetting, occurring as a function of temperature [27]. Recently Muolo *et al.* [28] found that, while ZrB_2 sintered from pure powder is not wetted by Ag and Cu (contact angles close to $125°$), very good wetting (contact angles close to $20°$) was observed with an addition to ZrB_2 of 4 wt% Ni as a sintering agent.

For compounds with a certain range of stoichiometry, a deviation of the surface from the bulk stoichiometry can be produced during the substrate preparation procedure (cutting, polishing). For instance, the formation on sintered, nominally stoichiomentric TiN of a surface layer hypostoichiometric in N_2 several tens of nm thick (Fig. 5) is responsible of the contact angle close to $60°$ observed for this ceramic (see Table II). Indeed, when a gas mixture containing N_2 is used to ensure an *in situ stochiometric* TiN surface, the contact angle increases by $35°$.

From the above it appears that, when only sintered materials are available for Young contact angle measurements, a particular effort has to be made with modern techniques (XPS, Auger spectroscopy...) to characterise their surface chemistry both before and after the wetting experiments. As for the topological characteristics of the surfaces (R_a, λ_a, average surface slope, etc.), common mechanical profilometers provide this information by analysing large areas (several mm^2).
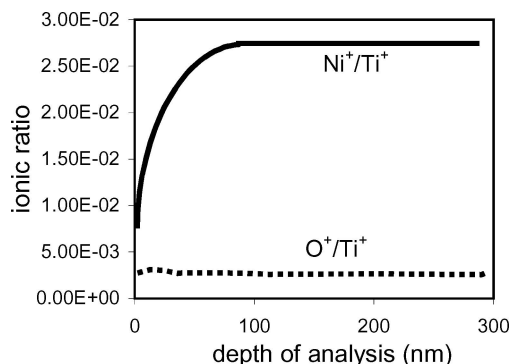

Figure 5 SIMS analysis of nominally stoichiometric TiN showing the relative intensity N^+/Ti^+ and O^+/Ti^+ as a function of depth [12].

This point is important in wetting experiments since millimeter-sized droplets are used. Simple optical microscopy is often sufficient to identify the presence of local defects such as scratches or pores. The shape of these defects can be obtained by AFM. Whatever the quality of the substrate, mono- or polycrystalline, several sessile drop experiments have to be carried out to ensure repeatability.

4. The effects of furnace atmosphere

The second major cause of scattering of contact angle data is pollution from the atmosphere, mainly oxygen. This element can lead to the formation of oxide skins on metallic droplets as well as on metallic or ceramic solids.

When thick oxide films are formed on a sessile drop, oxidation is evident because at melting, the surface of the liquid is not smooth. However, thin oxide skins of up to a few tens of nanometers are easily deformable, allowing a smooth surface to be formed. Yet, even very thin skins do not allow the metal/substrate interface to be formed and, as a result, the apparent contact angles are much higher than $90°$.

A classical example is pure Al, which at room temperature is instantaneously covered by an oxide layer of alumina about 2 nm thick resulting in large obtuse apparent contact angles on many ceramics. On heating Al on an alumina substrate at $T > T^*$, where T^* is 700–1000°C depending on the vacuum level in the furnace and the "quality" of the vacuum, i.e. the Po_2 value, a decrease in the contact angle towards a value close to $90°$ is observed due to deoxidation. This occurs mainly by reaction between Al and $Al_2O_3^{(skin)}$ with the formation of volatile Al_2O [14, 29]: $Al_2O_3^{(skin)} + Al^{(liquid)} = Al_2O\uparrow$. The necessary condition for this reaction to occur is that the partial pressure of oxygen in the furnace must be lower than the partial pressure of Al suboxide produced by the reaction. For a given value of Po_2, this is favoured by (i) a high temperature, which increases the equilibrium value of Al_2O, (ii) by the use of high vacuum, which promotes rapid evacuation of the Al_2O molecules far from the droplet surface, (iii) and when Al is alloyed with other elements, by a high thermodynamic activity of Al in the melt. The removal of oxide films may be also achieved by *in situ* Ar^+ ion sputtering [30] or by mechanical disruption when the liquid drop is dispensed onto the substrate surface through a small hole in a tube end (Fig. 1b).

Table IV presents the results for Al and Al alloys on Al_2O_3 obtained at $T < T^*$ both by the classical sessile drop and by the dispensed drop techniques. In all cases the dispensed drop technique leads to contact angles that are lower by several decades of degrees. It is interesting to notice that the formation of oxide skins occurs not only on alloys that are rich in oxidisable metals such as Al or Si, but also on alloys with low contents of these metals, such as Cu−Al [13] or Au−Si [34]. In these alloys the oxidisable metal is present in a concentration sufficient to produce oxidation at $T < T^*$ but too low to produce deoxidation at $T > T^*$. This causes a shift of T^* to higher temperatures, as discussed

TABLE IV Contact angles of pure Al and Al and Cu alloys on alumina measured by the classical sessile drop (SD) and the dispensed drop (DD) techniques

| Couple | Conditions | Contact angle, $\theta(°)$ | | Ref. |
		SD	DD	
Al/Al$_2$O$_3^{SC}$	Ar + 2%H$_2$; 700°C	125	104 (80^a)	Shen *et al.*, 2004 [31]
Al/Al$_2$O$_3^{PC}$	hv; 680°C	122	94	Sobczak, 2003 [32]
	1023°C	121	80	
AlTi6/Al$_2$O$_3^{PC}$	hv; 850°C	118	103	Sobczak, 2004 [33]
AlSi12/Al$_2$O$_3^{PC}$	hv; 700°C	122	98	
Cu-5 at% Al/Al$_2$O$_3^{SC}$	hv; 1150°C; 5 min	150	104	SD: Li *et al.* 1988 [3] DD: Eustathopoulos *et al.*, 1999 [13]

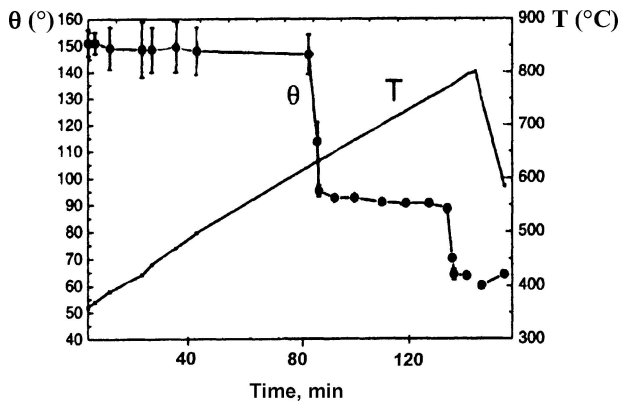^{a}A drop falling down from a height of 10 mm.

Figure 6 Contact angle of Pb on stainless steel as a function of time during a temperature cycle in high vacuum studied by the sessile drop method [35].

in [3]. The above results can explain easily the high inter-laboratory dispersion of θ_a values for Al alloys, especially at temperatures lower than 1000°C.

Contact angles as high as 150° are also observed for low melting-point metals such as Pb, Sn or In at temperatures close to their melting point. An example is molten Pb on FeCr martensitic steel (Fig. 6). As for Al, the surface of steels at room temperature is covered by an oxide layer a few nm thick, as evidenced by XPS analysis. The θ vs time curve obtained during continuous heating in a high vacuum shows three steady contact angles. By performing further experiments on steel with the dispensed drop technique to disrupt any oxide skin on the droplet and various heat treatments to deoxidise its surface *in situ*, Protsenko *et al.* [35] showed that the large obtuse angles observed at low temperature are apparent contact angles due to Pb oxidation. The contact angles close to 90° (domain B) and 60° (domain A) are true contact angles for deoxidized Pb on oxidized and deoxidized (metallic in character) steel surfaces, respectively.

This example illustrates a long-known fact: skin oxides on metallic solids act as barriers to wetting by molten metals [1, 36, 37]. Such oxide films can also grow on many non-oxide but oxidisable ceramics such as SiC, Si$_3$N$_4$, AlN. In a recent study [38] it was found, by combining wetting experiments and surface analysis by Auger and XPS, that in a high vacuum environment at temperatures lower than about 1000°C the chemistry

of the outer surface of SiC is close to that of silica. As a result, the contact angles for low-melting point metals such as In, Ga or Sn on SiC are expected (and indeed found) to be close to those on SiO$_2$, i.e., in the range 120–130°. Similar phenomena may occur on other non-oxide ceramics such as Si$_3$N$_4$, AlN or TiN. Oxidation of TiN, together with roughness, may explain the highest contact angles in Table II.

At high temperature or in a low P_{O_2} atmosphere, oxide films are often eliminated by thermodynamic decomposition or by formation of volatile sub-oxides. Even in these situations, oxygen dissolved in the liquid metal can still affect the wettability of a metal/oxide system at both "high" and low P_{O_2} values. This is illustrated schematically in Fig. 7 for a metal M/alumina couple. For usual metals such as Pb, Sn, In, Bi, Ge, Ag, or Cu, the contact angle is independent of P_{O_2} in a wide range of oxygen partial pressure. At very low P_{O_2}, dissolution of alumina into the liquid metal will occur in order to satisfy the equilibrium Al$_2$O$_3$ → 2(Al)M + 3/2O$_2$. Then the equilibrium angle starts to decrease with decreasing P_{O_2} (or, equivalently, with an increasing concentration of Al in the metal), a behaviour that is typical of M-Al alloys [13]. Above a certain partial pressure $P_{O_2}^*$, the value of which is a function of the metal and of the temperature, the contact angle starts to decrease again due to adsorption of oxygen at the metal/vapour and metal/oxide interfaces.
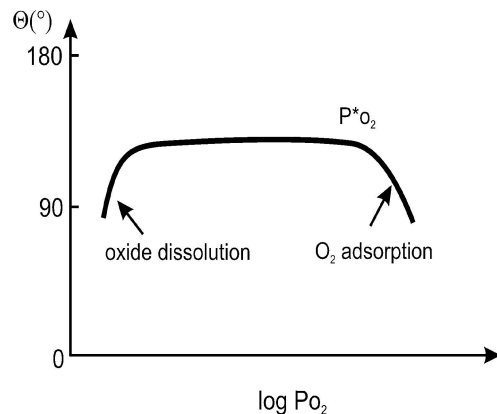

Figure 7 Schematic representation of contact angle *vs* logP_{O_2} for a pure metal on an ionocovalent oxide at constant T. At the high P_{O_2} limit the adsorption domain is limited by the oxidation of the metal [13,24].
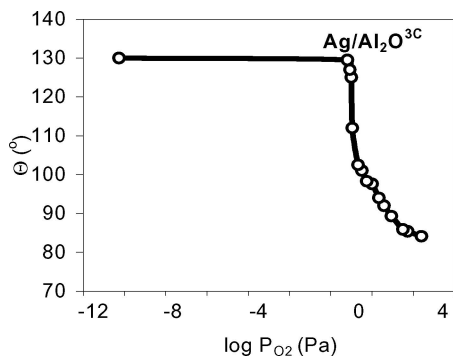
Figure 8 The variation of contact angle of Ag on $Al_2O_3^{SC}$ with the logarithm of partial pressure of oxygen at 980°C [36].

An example is given in (Fig. 8) for Ag/alumina couple. As the partial pressure of oxygen in the furnace increases, the contact angle remains nearly constant, then decreases sharply at Po_2^* and tends more slowly towards 80°. The threshold pressure in this example is about 10^{-4} atm, but it is about 10^{-12} atm for Cu on alumina at 1100°C [40] and only 10^{-18} atm for Pb on SiO_2 at 673°C [41].

While Po_2 values lower than 10^{-4} atm can be easily obtained in moderate-quality equipment using, for instance, common purity neutral gases, Po_2 values lower than 10^{-10} atm need particular care, as will be discussed in the next paragraph. For this type of system, the experimental results obtained by different teams in different (but not quantified) Po_2 environments can produce a further dispersion of contact angles in the "same system". Note that for high melting-point metals such as Ni and Fe on alumina, the decrease in thermodynamic stability of alumina caused by the high temperature and the strong Ni-Al (and Fe-Al) interactions transform the wetting plateau of Fig. 7 to a simple maximum (Fig. 9). Clearly, for this system, an "intrinsic" contact angle has no sense without specifying the Po_2 value during the experimental run. The curve of Fig. 9 helps to explain a large part of the particularly wide scatter of the experimental data observed for this system (see introduction) as all the contact angles between 127° and 104° are permitted when the content of oxygen in Ni changes from a few ppm to 50 ppm.

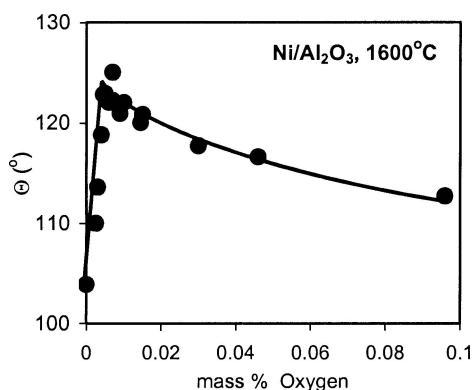In order to obtain low Po_2 environments, wetting experiments are usually carried out by employing inert

Figure 9 Contact angle of Ni on Al_2O_3 vs oxygen content in Ni at 1600°C [42].

gases or high vacuum. Common inert gases contain a few ppm of oxidizing gases such as O_2 and H_2O, which correspond to $Po_2 \approx 10^{-5}$–10^{-6} atm in 1 atm of gas. This Po_2 is sufficient to cause oxidation of many common pure metals at their melting point and, except for Ag on ionocovalent oxides, it is higher than the Po_2^* defining the beginning of the oxygen-wetting transition on oxides. It is a good practice, therefore, to purify inert gases by pressing them slowly over heated powder or shavings of a reactive metal such as Ti, Zr or Mg. An alternative solution is to mix a small amount, typically a few percent, of H_2 with the inert gas. In some furnaces, graphite is present inside the chamber as a heating element or is placed near the testing couple in order to reduce Po_2 [19, 43], a practice used in metallurgy for decades [44]. This indeed helps to lower the Po_2 values but may also cause contamination of the droplet and of the substrate by C. In many cases this is not a serious problem because even limited solubility of carbon in the droplet or in the substrate allows this element to be removed from the surface by diffusion towards the interior of bulk phases. Note that, as a rule, dissolved carbon is not an "active" element at the surfaces and interfaces of high-temperature materials. However, if the solubility is too low, carbon layers can be formed and influence wetting. For instance, it has been found that carbon layers a few nm thick improve the wetting of alumina by molten aluminium [45, 46]. In another example Rado [19] found that the spreading time (but not the final contact angle) of CuSi alloys on SiC in a metallic furnace was increased by an order of magnitude when the experiment was repeated in an alumina furnace inside which a graphite tube was placed to avoid oxidation of SiC. In order to reveal possible *in situ* contamination by C of SiC substrates, Rado placed a Si wafer inside the graphite tube. Even a few minutes of heating at 1100°C were enough to observe Auger spectra typical of SiC on the Si surface after cooling. Using SEM it was even possible to distinguish the SiC particles growing on the Si surface by reaction between Si and C.

Some research groups prefer to use high vacuum because it promotes evaporation and dissociation of oxide films on the liquid or substrate surfaces by forming volatile sub-oxides, as discussed above. However, when the vapour pressure of the liquid is high, evaporation may reduce the volume of the drop. On rough surfaces this produces an apparent decrease in θ with time, which actually is due to a gradual change in contact angle from advancing to receding. This artifact can easily be detected by measuring not only θ but also the linear dimensions of the droplet (drop base diameter and drop height). When the vacuum is obtained by oil diffusion pumped systems, the effective Po_2 value may be several orders of magnitude smaller than the total pressure because of the reducing atmosphere generated by cracked oil molecules. However, this cracking may also contaminate the droplet and the substrate with C, which can be reduced but not suppressed by using liquid N_2 traps. For this reason, more and more high-temperature devices employ oil-free equipment such as turbo-molecular pumps.

5. From contact angles to work of adhesion

The surface tension of high-temperature melts (liquid metals and alloys, glasses, salts) can be measured by several techniques: (i) Surface shape methods (sessile drop and pendant drop), (ii) Capillary Pressure Methods (pressure derivative, expanded drop, maximum bubble pressure), (iii) Oscillating-levitating drop and (iv) Drop weight [47]. All require careful preparation and control of each experiment, full knowledge of all the physico-chemical parameters of the system under study, and careful interpretation of the phenomena occurring between the liquid metal surface, the gaseous environment and the solid surface eventually in contact with the melt: metal evaporation, bulk diffusion, surface adsorption, chemical reactions in the gas phase, mass transfer, competition between diffusion and kinetics of the gaseous species under the different experimental environments (e.g. inert gas or vacuum), and chemical reactivity with reference to competitive bulk and surface reactions [48]. Theoretical models have been developed taking into account all these effects, allowing the best working conditions to be singled out and the oxygen behaviour including its actual partial pressure near the liquid surface to be predicted [49, 50].

To get meaningful values of the work of adhesion, the surface tension of the liquid phase must be evaluated when the liquid is in contact with the solid body, that is, in the same physico-chemical environment as that used to measure the contact angle. This allows, for example, any effect of interactions between the liquid and the solid on the surface tension to be taken into account. Although surface tension and contact angle can be measured simultaneously by the immersion-emersion tensiometric method [13], in the high-temperature range the sessile drop technique is used most often for this purpose. However, this method is really accurate for surface tension measurements only if the contact angle is larger than 90°, even though good results can also be obtained down to 60–70° provided special precautions are taken.

If the contact angle is less than 90°, one solution is to measure the surface tension using a cup of the same material for which the contact angle has to be evaluated ("large drop" [51] or, better, "pinned-sessile drop" method [47], which may be used also with small drops). Another possibility is to use the immersion-emersion tensiometric method mentioned above, which can be applied for both wetting and non-wetting systems. Finally, it is also possible to try to equilibrate the liquid in contact with the solid under investigation, and then to measure the "contaminated liquid" surface tension by some other method (pendant drop, sessile drop on inert substrate, capillary pressure etc.).

In contrast, with large contact angles (>150°), the gap between the solid surface and the drop profile just near the boundary triple line becomes increasingly narrow. Especially at high temperatures, unwanted reflections, optical distortions, together with the unavoidable lack of focusing sharpness (which is also due to the fact that the meridian drop section has at least half of the solid support surface in front of it) blur the image exactly in the measuring zone, thus making it difficult if not impossible to determine the contact point with sufficient precision and then to "draw" the tangent line. A quantitative evaluation shows that errors up to 5–10° are easily possible in this range.

Generally, if the position of the surface of contact can be determined with sufficient precision, the entire surface tension measurement procedure, based on the fitting of the Laplace equation [48, 52], often performed by automatic imaging procedures [53], also gives a reliable value of contact angle value.

Finally, a typical difficulty comes from the high-temperature environment: above 1000°C light emission is very strong, with an emission spectrum shifting from the infrared region towards the blue wavelength. This means that the energy hitting the CCD elements is not constant. This causes a continuous shift in their response, which in turn makes it impossible to maintain a constant image quality. Thus, infrared and other filters have to be used; however a good solution is to cut the emission of the drop itself completely by ad-hoc filters and to use a very strong backlight source. In this way, constant imaging conditions can be obtained.

6. Conclusions

During the last 20 years there has been a great improvement in the measurement of contact angles of high-temperature systems. A major reason for this has been the use of monocrystalline or vitreous solids to prepare the high-quality surfaces required for meaningful Young contact angle determinations. In this period, wetting studies have also benefited from high-resolution techniques for characterising the topological and chemical features of surfaces at a nanometric scale. Further improvement is expected in the next few years through the introduction of ultra-high vacuum standards and through the use of the more sophisticated versions of the sessile drop method (dispensed drop, transferred drop) enabling *in situ* cleaning of surfaces. In all cases, an automatic system for data acquisition and image analysis enabling the simultaneous measurement of contact angle and surface tension, is desirable. For certain ceramics, which are hardly available as monocrystalline material but have a high technological interest (many carbides, nitrides, borides, etc.), a semi-quantitative evaluation of their wetting and adhesion properties with metals is possible. However, this needs a high number of sessile drop experiments to prove acceptable repeatability, as well as detailed characterisation of their surface chemistry both before and after the wetting experiment.

A resume of main requirements for the experimental evaluation of intrinsic contact angles is given in the Appendix.

Appendix

Requirements for Young contact angle measurements

The experimental evaluation of reliable contact angles to be used in Young equation and to calculate the work of adhesion, requires a careful control of the experimental conditions and of the topology and chemistry of the substrates.

In particular the following steps should be followed with rigorous attention:

(1) The chemical composition of the solid and liquid components should be explicitly given.

(2) The surface roughness has to be quantified: substrates with r_a values lower than 100 nm must be used in order to achieve an acceptable accuracy on θ (a few degrees).

(3) The characterization of substrate surface chemistry before and after the wettability experiment is often necessary in order to identify clearly the meaning of the measured contact angle.

(4) The wettability experiments must be conducted in controlled furnace conditions obtained either by high vacuum or, if in the presence of gases, by measuring the partial pressure or concentration of each reactive impurity, especially of oxygen.

(5) Although, as a general rule, advancing contact angles are involved in wetting experiments, only the simultaneous inspection of $\theta(t)$, $R(t)$ and $h(t)$ curves allows to confirm this feature.

(6) When using automatic techniques based on image-analysis softwares, the contact angle could be derived from the solution of the Laplace equation, provided the drop has a shape factor larger than 2; if a portion of the drop close to the triple line is used, taking care that the number of coordinate points used is large enough to warrant a sufficient statistical accuracy. Evidence should be offered, at least with a check on the solidified drop, that an axisymmetric profile has been retained during the experiment.

(7) When computing the Work of Adhesion W_a, the necessary contact angle and surface tension values must be measured in the same conditions and, if possible, using the same substrate.

References

1. Y. V. NAIDICH, "The Wettability of Solids by Liquid Metals, Progress in Surface and Membrane Science", edited by D. A. Cadenhead and J. F. Danielli (Academic Press, NY, (1981)**14**, p. 353.
2. P. D. OWNBY and J. LIU, *J. Adhesion Sci. Technol.* **2** (1988) 255.
3. J. LI, L. COUDURIER, I. ANSARA and N. EUSTATHOPOULOS, *Ann. Chim. Fr.* **13** (1988) 145.
4. V. DE JONGHE, D. CHATAIN, I. RIVOLLET and N. EUSTATHOPOULOS, *J. Chim. Phys.* **87** (1990) 1623.
5. P. VIKNER, *DEA report*, LTPCM, INP Grenoble, France (1993).
6. V. GHETTA, J. FOULETIER and D. CHATAIN, *Acta Mater.* **44** (1996) 1927.
7. E. SAIZ, A. P. TOMSIA and R. M. CANNON, *ibid.* **46**(7) (1998) 2349.
8. H. KOTSCH, *Neue Hütte* **12** (1967) 350.
9. P. XIAO and B. DERBY, *J. Mater. Sci.* **30** (1995) 5915.
10. S. LEQUEUX, F. LE GUYADEC, M. BERARDO, L. COUDURIER and N. EUSTATHOPOULOS, in Proc. 2nd Int. Conf. on High Temeperature Capillarity, edited by N. Eustathopoulos and N. Sobczak (Foundry Research Institute, Cracow, Poland, 1998) p. 112.
11. M. L. MUOLO, M. BASSOLI, B. WOLLEIN, W. LENGAUER and A. PASSERONE, *Trans. JWRI* **30** (2001) 49.
12. S. KALOGEROPOULOU, J. VAN DEELEN, N. EUSTATHOPOULOS, F. LE GUYADEC and M. BERARDO, *ibid.* **30** (2001) 107.
13. N. EUSTATHOPOULOS, M. G. NICHOLAS and B. DREVET, "Wettability at High Temperature", Pergamon, Pergamon Materials Science Series (1999) Vol **3**.
14. V. LAURENT, D. CHATAIN, M. CHATILLON and N. EUSTATHOPOULOS, *Acta Metall.* **36** (1988) 1797.
15. N. SOBCZAK, M. KSIAZEK, W. RADZIWILL, L. STOBIERSKI and B. MIKULOWSKI, *Trans. JWRI* **30** (2001) 125.
16. R. SHUTTLEWORTH and G. BAILEY, *Discuss. Faraday Soc.* **3** (1948) 16.
17. S. J. HITCHOCK, N. T. CARROL and M. G. NICHOLAS, *J. Mater. Sci.* **16** (1981) 714.
18. Y. V. NAIDICH, R. P. VOITOVICH, G. A. KOLESNICHENKO and B. D. KOSTYUK, *Adgezia Rasplavov i Payka Materialov* **19** (1987) 23.
19. S. RADO, Ph.D. Thesis, INP Grenoble, France (1997).
20. J. BRENNAN and J. PASK, *J. Amer. Cer. Soc.* **51** (1968) 569.
21. R. SANGIORGI, M. L. MUOLO, D. CHATAIN and N. EUSTATHOPOULOS, *J. Amer. Ceram. Soc.* **71** (1988) 742.
22. J. LI, Ph. D. Thesis, INP Grenoble, France (1988).
23. P. NIKOLOPOULOS, S. AGATHOPOULOS, G. N. ANGELOPOULOS, A. NAOUMIDIS and H. GRUBMEIER, *J. Mater. Sci.* **27** (1992) 129.
24. E. SAIZ, R. M. CANNON and A. P. TOMSIA, *Acta Mater.* **47** (1999) 4209.
25. Y. NAIDICH, R. VOITOVICH and V. ZABUGO, *J. Colloid Interf. Sci.* **174** (1995) 104.
26. V. DE JONGHE and D. CHATAIN, *Acta Met. Mater.* **43** (1995) 1505.
27. M. BRUNET, Ph. D. Thesis, INP, Grenoble, France (1973).
28. M. L. MUOLO, E. FERRERA, R. NOVAKOVIC and A. PASSERONE, *Scripta Mater.* **48** (2003) 191.
29. P. CASTELLO, E. RICCI, A. PASSERONE and P. COSTA, *J. Mater. Sci.* **29** (1994) 6104.
30. G. LEVI and W. D. KAPLAN, *Acta Mater.* **50** (2002) 75.
31. P. SHEN, H. FUJII, T. MATSUMOTO and K. NOGI, *J. Amer. Cer. Soc.* **87**(7) (2004) 1265.
32. N. SOBCZAK, *Kompozyty* **3**(7) (2003) 301.
33. N. SOBCZAK, *Ceram. Trans.*, **146** (2004) 83.
34. B. DREVET, D. CHATAIN and N. EUSTATHOPOULOS, *J. Chim. Phys.* **87** (1990) 117.
35. P. PROTSENKO, A. TERLAIN, M. JEYMOND and N. EUSTATHOPOULOS, *J. Nucl. Mater.* **307–311** (2002) 1396.
36. A. BONDI, *Chem. Rev.* **52** (1953) 417.
37. B. MCGURRAN and M. G. NICOLAS, *Brazing and Soldering* **8** (1985) 43.
38. C. RADO and N. EUSTATHOPOULOS, *Inter. Sci.* **12** (2004) 85.
39. B. GALLOIS, Ph.D. Thesis, Carnegie Mellon Univ., Pittsburgh, USA, 1980.
40. D. CHATAIN, F. CHABERT, V. GHETTA and J. FOULETIER, *J. Am. Ceram. Soc.* **77** (1994) 197.
41. N. EUSTATHOPOULOS, B. DREVET and M. L. MUOLO, *Mat. Sci. Eng.* **A300** (2001) 34.
42. K. NOGI, N. IWAMOTO and K. OGINO, *Trans. JWRI* **21** (1992) 141.
43. N. FROUMIN, N. FRAGE, M. POLAK and M. P. DARIEL, *Acta Mater.* **48** (2000) 1435.
44. "Vacuum Technology—Practical Heat Treating and Brazing", edited by R. Fabian (ASM International, Ohio, USA, 1993) p. 21.
45. H. JOHN and H. HAUSNER, *Int. J. High Tech. Ceram.* **2** (1986) 73.
46. D. A. WEIRAUCH and W. J. KRAFICK, *Met. Trans.* **21A** (1990) 1745.
47. A. PASSERONE and E. RICCI, in "Drops and Bubbles in Interfacial Research", edited by D. Möbius and R. Miller (Elsevier, 1998) p. 475.

48. P. COSTA, E. RICCI and PASSERONE, *High Temp. High Press.* **20** (1998) 59.
49. M. RATTO, E. RICCI and E. ARATO, *J. Cryst. Growth* **217** (2000) 233.
50. M. RATTO, E. RICCI and E. ARATO and P. COSTA, *Metall. Mater. Trans.* **32B** (2001) 903.
51. Y. NAIDICH, V. EREMENKO, V. FESENKO, M. VASILIU and L. KIRICHENKO, in "The Role of Surface Phenomena in Metallurgy", edited by V. Eremenko (Consultants Bureau, New York, 1963) p. 41.
52. F. BASHFORTH and C. ADAMS, "An Attempt to Test the Theories of Capillary Action", (Cambridge Univ. Press, 1883).
53. L. LIGGIERI and A. PASSERONE, *High Temp. Tech.* **7** (1989) 80.